View metadata, citation and similar papers at core.ac.uk
brought to you by CORE
provided by Open Archive Toulouse Archive Ouverte

Launcher attitude control: discrete-time robust design and gain-scheduling

Olivier Voinot[a], Daniel Alazard[b,*], Pierre Apkarian[c], Sophie Mauffrey[d], Benoît Clément[e]

[a] ONERA-CERT, Control System Dept., 2 av. Edouard Belin, 31055 Toulouse, France
[b] SUPAERO, System Dynamics and Control, 10 av. Edourd Belin - BP.4032, 31055 Toulouse, France
[c] ONERA-CERT, Control System Dept., 2 av. Edouard Belin, 31055 Toulouse, France
[d] EADS/LV, 66 Route de Verneuil, Les Mureaux, France
[e] CNES/DLA, Rond Point de l'Espace, 91023 Evry Cedex, France

Abstract

In this paper, a robust multi-objective design for the control of a launcher during atmospheric flight is investigated. This approach is based on the Cross Standard Form formulation which allows to incorporate the various specifications of the launcher problem in a streamlined manner. An important feature of this approach is that a non-conventional LQG/LTR approach, required to satisfy time-domain specifications, can be embedded into a more general standard problem in order to account for frequency-domain robustness constraints. The specific form of this standard problem is also very interesting for gain scheduling.

Keywords: Multi-objective design; Robustness; Cross standard form; Launcher; Gain scheduling

1. Introduction

This article presents the discrete-time version of a new method for multi-objective synthesis presented in Voinot, Alazard, Piquereau, and Biard (2001). This method is based on the Cross Standard Form (CSF) presented as a generalization of the LQ inverse problem to the H_2 and H_∞ inverse problems. Indeed, the CSF allows to formulate a standard problem from which an initial compensator can be obtained by H_2 or H_∞ synthesis. The demonstration of the properties of the CSF is based on the possibility to determine the *minimal* observer-based realization of arbitrary compensator (Alazard & Apkarian, 1999). From a practical point of view, the CSF is used to mix various synthesis techniques in order to satisfy a multi-objective problem. The general idea is to perform a first synthesis to reach some specifications, mainly performance specifications. Then, the CSF is applied to this first solution to initialize a standard problem which will be gradually completed to handle frequency-domain or parametric robustness specifications. This approach is particularly interesting when the designer wants to:

- take advantage of an initial compensator based on a priori know-how and physical considerations, and
- exploit modern optimal control techniques to deal with frequency-domain robustness specifications and trade-offs between various specifications.

Other potentialities of this approach, like mixed eigenstructure assignment/H_∞ control or multi-channel control, are proposed in Alazard and Voinot (2002) and Alazard (2002). See also Apkarian, Tuan, and Bernussou (2001) for an alternative approach.

In this paper, the low-level control loop of a non-stationary launcher during atmospheric flight is considered. Only the yaw attitude is explored: the problem is formulated in terms of angle-of-attack regulation in face of a typical wind profile (disturbance rejection problem) and consumption reduction. Robustness specifications are expressed in the frequency domain for a set of operating instants regularly spaced along the

*Corresponding author. Tel.: +33-5-62-17-80-94; fax: +33-5-62-17-83-45.
E-mail address: alazard@supaero.fr (D. Alazard).

flight path: the open loop transfer ($L(s) = K(s)\ G(s)$) must satisfy templates on the NICHOLS chart for various critical configurations sampled in the uncertain parameter space. Uncertain parameters are the main dynamic parameters on the rigid mode (aerodynamic coefficient, thruster efficiency, etc.) and on the bending modes (natural frequencies, modal participation factors).

Considering the pure stationary synthesis problem at one flight instant, there is no method, to our knowledge, that can handle a set of specifications (time-domain performance and open-loop frequency-domain specifications) in a streamlined manner. Multi-objective optimization can be used in conjunction with frequency-domain design (for instance, genetic algorithms and H_∞ design in Griffin, Schroder, Chipperfiled, and Fleming (2000)) but these approaches might be costly in terms of computational time. Although our approach is also indirect, its capability to take advantage of know-how is particularly highlighted in this application: the time-domain performance specification (angle-of-attack peak amplitude in response to typical wind profiles) is handled by a non-conventional LQG synthesis in which the LQ state feedback is computed in a two-step procedure based on physical considerations. Then, this synthesis is incorporated into a standard H_∞ problem in order to meet frequency-domain templates. The final H_∞ synthesis meets all the specifications and produces, a low-order compensator in comparison with alternative approaches applied on the same problem (Mauffrey & Scholler, 1998; Clément & Duc, 2000; Clément, Duc, Mauffrey, & Biard, 2001).

In a sense, this approach can be seen as a competitive method for mixed H_2/H_∞ synthesis problems for which an extensive literature has appeared in the last decade (Doyle, Zhou, Glover, & Bodenheimer, 1994; Fan, Cliff, Lutze, & Anderson, 1996; Shue & Agarwal, 1999). But the main practical problem with all optimal approaches is the expression of specifications as the minimization of a closed-loop transfer with respect to a particular norm.

All the design is conducted in discrete-time. In comparison with our previous paper (Voinot et al., 2001) devoted to the continuous-time case, it is important to note that the phase shift introduced by the zero-order hold is now taken into account in the synthesis model. The control law design is then significantly simplified: the first-order phase lead required in Voinot et al. (2001) to meet the delay margin is no longer of any use and the trade-off between low frequency stability margins and roll-off requirement on flexible modes is somewhat relaxed.

Considering the non-stationary problem, the stationary compensators synthesized by our approach at each flight instant need to be interpolated. It is well known that the non-stationary behavior of interpolated control laws depends strongly upon compensator realizations which are interpolated. Observer-based realizations are very attractive from the gain-scheduling point of view (Stilwell & Rugh, 1999; Pellanda, Apkarian, & Alazard, 2000). The main reason is that the compensator states are consistent and have physical units if the model on which the observer-based realization is built, has physical states. Another important feature of the proposed approach is that the final H_∞ problem is a pure Disturbance Feed-forward problem (Zhou, Doyle, & Glover, 1996). It follows that the DGKF (Doyle, Glover, Khargonekar and Francis) central solution (Doyle, Glover, Khargonekar, & Francis, 1989) has a pure observer-based structure. This is however not the case when Linear Matrix Inequality techniques are used to solve the H_∞ control problem since compensator realizations are entirely out of control and techniques such as those in Alazard and Apkarian (1999) must be used to restore an observer-based realization.

In the first part of this paper, the discrete-time version of the CSF is presented. In the second part, launcher model and specifications are described. In the third part, the application of the CSF method and the whole stationary design procedure are detailed. The last part is dedicated to the gain scheduling of the various compensators to solve the non-stationary problem.

Standard notations

A^{T}	Transpose of matrix A
$\dot{x}$	Time derivation ($\dot{x} = \partial x/\partial t$)
s	LAPLACE variable
T_S	Sampling period
x_k	Discrete-time value of x ($x(t)\|_{t=kT_S}$)
z	Delay operator
$G(\delta) := \left[\begin{array}{c\|c} A & B \\ \hline C & D \end{array}\right]$	State-space realization of transfer $G(\delta) : G(\delta) = D + C(\delta I - A)^{-1} B (\delta = s \text{ or } z)$
$P = \begin{bmatrix} P_{qe} & P_{qu} \\ P_{ye} & P_{yu} \end{bmatrix}$	General standard problem between exogenous input e, actuator signal u, regulated output q and measurement y
$\left[\begin{array}{c\|c\|c} A & B_1 & B_2 \\ \hline C_1 & D_{11} & D_{12} \\ \hline C_2 & D_{21} & D_{22} \end{array}\right]$	Shorthand for state-space realization of $P(s)$
$F_l(P, K)$	Lower Linear Fractional Transformation of P and K

Acronyms

CSF	Cross Standard Form
LQ	Linear Quadratic
LQG	Linear Quadratic Gaussian
LTR	Loop Transfer Recovery
DGKF	Doyle, Glover, Khargonekar and Francis

2. The Cross Standard Form

2.1. *General inverse problem statement and definitions*

Consider a stabilizable and detectable system $G(z)$ with minimal state-space realization (n states, m inputs, p outputs):

$$\begin{bmatrix} x_{k+1} \\ y_k \end{bmatrix} = \left[\begin{array}{c|c} A & B \\ \hline C & D \end{array}\right] \begin{bmatrix} x_k \\ u_k \end{bmatrix} \tag{1}$$

Consider also a n_Kth order stabilizing compensator $K_0(z)$ (with $n_K \geqslant n$).

Definition 2.1 (H_2 Inverse problem). Find a n_Kth order standard problem $P(z)$ such that $P_{yu}(z) = G(z)$ and

$$K_0(z) = \arg\min_{K(z)} \|F_l(P(z),\ K(z))\|_2$$

(that is: $K_0(z)$ minimizes $\|F_l(P(z),\ K(z))\|_2$).

Definition 2.2 (H_∞ inverse problem). Find a n_Kth order standard problem $P(z)$ such that $P_{yu}(z) = G(z)$ and

$$K_0(z) = \arg\min_{K(z)} \|F_l(P)(z),\ K(z))\|_\infty.$$

Definition 2.3 (Cross Standard Form). If the standard problem $P(z)$ is such that $P_{yu}(z) = G(z)$ and

$$F_l(P(z), K_0(z)) = 0$$

then $P(z)$ is called a Cross Standard Form associated with the system $G(z)$ and the compensator $K_0(z)$.

Of course, the CSF solves the H_2 inverse problem and the H_∞ inverse problem.

2.2. *An observer-based solution*

LQG compensator or more generally compensators involving a state observer (with an estimation gain K_f), a state feedback (with a gain K_c) and a dynamic YOULA's parameter Q are quite interesting to build a CSF (Voinot et al., 2001). In discrete-time, one can distinguish 2 LQG structures: the predictor structure and the estimator structure (see Alazard and Apkarian (1999) for more details). The discrete predictor LQG structure, and the YOULA parameterization of all stabilizing compensators based on it, are analogous to the continuous-time case. All the results presented in this paper concern the discrete estimator LQG structure. Indeed, from a practical point of view, the discrete-time KALMAN filter uses the last measurement y_k at the time $t=kT_s$ to update the estimated state $\hat{x}_k$. Then, the LQG compensator built on a such KALMAN filter exhibits a direct feed-through. This is the major difference between discrete-time LQG synthesis and discrete-time H_2 synthesis. This difference does not occur in continuous time. The structure of a such LQG compensator is depicted in Fig. 1. Also recall that this structure allows to parameterize all stabilizing compensators. The

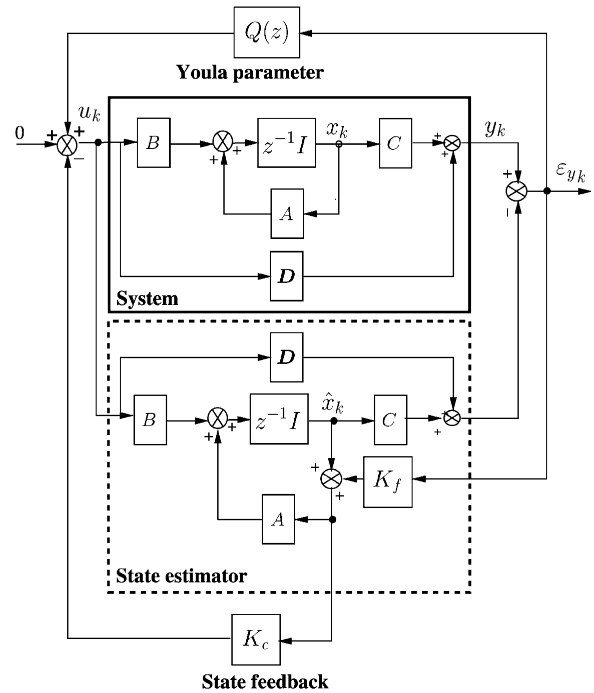

Fig. 1. The discrete YOULA parameterization on the estimator LQG structure.

authors in Alazard and Apkarian (1999) proposed a procedure to compute the parameters K_c, K_f and $Q(z)$ which characterize this structure from a given n_Kth order compensator $K(z)$ and a given nth order system $G(z)$ (with: $n \leqslant n_K$). This procedure will be very useful, in the following, to establish the CSF associated to an arbitrary compensator and in Section 5, to implement and interpolate various compensators with observer-based realizations.

The state-space representation of the compensator $K(z)$ associated with the structure depicted in Fig. 1 reads:

$$\begin{aligned} \hat{x}_{k+1} &= A\hat{x}_k + Bu_k + AK_f(y_k - C\hat{x}_k - Du_k), \\ x_{Q_{k+1}} &= A_Q x_{Q_k} + B_Q(y_k - C\hat{x}_k - Du_k), \\ u_k &= -K_c\hat{x}_k + C_Q x_{Q_k} + (D_Q - K_cK_f)(y_k - C\hat{x}_k - Du_k), \end{aligned} \tag{2}$$

where A_Q, B_Q, C_Q and D_Q are the four matrices of the state-space realization of $Q(z)$ associated to the state vector x_Q.

Proposition 2.4. *The CSF, $P(z)$, associated with the compensator defined by (2), such that*

$$F_l(P(z),\ K(z)) = 0 \tag{3}$$

reads

$$P(z) := \left[\begin{array}{cc|c|c} A & 0 & AK_f & B \\ 0 & A_Q & B_Q & 0 \\ \hline K_c & -C_Q & -D_Q + K_cK_f & I_m \\ \hline C & 0 & I_p & D \end{array}\right]. \tag{4}$$

The block diagram associated with this particular standard problem is depicted in Fig. 2.

Proof. Without loss of generality, assume $D = 0$. Consider the augmented notation:

$$\hat{x}^a = \begin{bmatrix} \hat{x} \\ x_Q \end{bmatrix}, \ A^a = \begin{bmatrix} A & 0 \\ 0 & A_Q \end{bmatrix}, \ B^a = \begin{bmatrix} B \\ 0 \end{bmatrix},$$

$$K_f^a = \begin{bmatrix} AK_f \\ B_Q \end{bmatrix}, \tag{5}$$

$$C^a = [C \ \ 0], K_c^a = [K_c - C_Q], D_Q^a = D_Q - K_c K_f \tag{6}$$

Then $P(z)$ and $K(z)$ read, respectively,

$$P(z): \left[\begin{array}{c} x^a_{k+1} \\ \hline q_k \\ \hline y_k \end{array}\right] = \left[\begin{array}{c|c|c} A^a & K^a_f & B^a \\ \hline K^a_c & -D^a_Q & I_m \\ \hline C^a & I_p & 0 \end{array}\right] \left[\begin{array}{c} x^a_k \\ \hline e_k \\ \hline u_k \end{array}\right], \tag{7}$$

$$K(z): \left[\begin{array}{c} \hat{x}^a_{k+1} \\ \hline u_k \end{array}\right] = \left[\begin{array}{c|c} A^a - B^a K^a_c - K^a_f C^a - B^a D^a_Q C^a & K^a_f + B^a D^a_Q \\ \hline -K^a_c - D^a_Q C^a & D^a_Q \end{array}\right] \times \left[\begin{array}{c} \hat{x}^a_k \\ \hline y_k \end{array}\right]. \tag{8}$$

The state-space representation of $F_l(P(z), K(z))$ can be written

$$\left[\begin{array}{c} x^a_{k+1} \\ \hat{x}^a_{k+1} \\ \hline q_k \end{array}\right] = \left[\begin{array}{cc|c} A^a + B^a D^a_Q C^a & -B^a K^a_c - B^a D^a_Q C^a & K^a_f + B^a D^a_Q \\ K^a_f C^a + B^a D^a_Q C^a & A^a - B^a K^a_c - K^a_f C^a - B^a D^a_Q C^a & K^a_f + B^a D^a_Q \\ \hline K^a_c + D^a_Q C^a & -K^a_c - D^a_Q C^a & -D^a_Q + D^a_Q \end{array}\right] \times \left[\begin{array}{c} x^a k \\ \hat{x}^a_k \\ \hline e_k \end{array}\right].$$

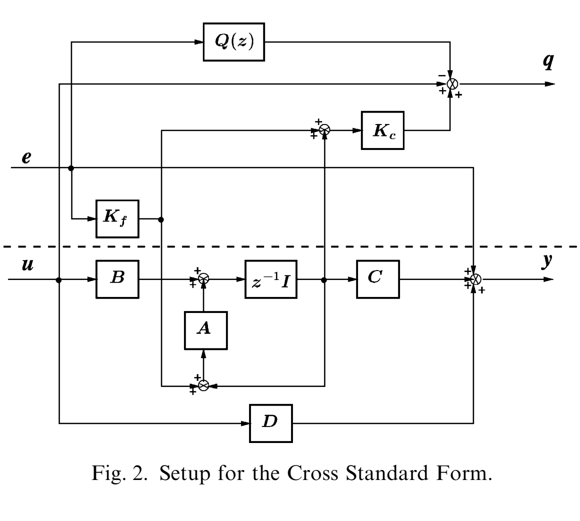

Fig. 2. Setup for the Cross Standard Form.

With the change of variable using the estimation error $\varepsilon^a_k = x^a_k - \hat{x}^a_k$ associated with the Kalman filter:

$$\begin{bmatrix} x^a_k \\ \hat{x}^a_k \end{bmatrix} = M \begin{bmatrix} x^a_k \\ \varepsilon^a_k \end{bmatrix} \text{ with } M = \begin{bmatrix} I_{n\times n} & 0 \\ I_{n\times n} & -I_{n\times n} \end{bmatrix} \text{ and}$$
$$M^{-1} = M, \tag{9}$$

the representation of $F_l(P(z), K(z))$ becomes

$$\left[\begin{array}{c} x^a_{k+1} \\ \varepsilon^a_{k+1} \\ \hline q_k \end{array}\right] = \left[\begin{array}{cc|c} A^a - B^a K^a_c & B^a K^a_c + B^a D^a_Q C^a & K^a_f + B^a D^a_Q \\ 0 & A^a - K^a_f C^a & 0 \\ \hline 0 & K^a_c + D^a_Q C^a & 0 \end{array}\right] \times \left[\begin{array}{c} x^a_k \\ \varepsilon^a_k \\ \hline e_k \end{array}\right]. \tag{10}$$

One can observe here that the states ε^a_k associated with the estimation error are uncontrollable by e_k and that the states x^a_k of the plant are unobservable by q_k. The transfer between e_k and q_k is thus null:

$$F_l(P(z), K(z)) = 0 \quad \square \tag{11}$$

Practical use: The CSF brings the possibility to formulate the standard problem on which the H_2 and H_∞ synthesis allow to compute the initial compensator. This result can be considered as a generalization, for H_2 and H_∞ criteria and for dynamic output feedbacks, of the solution to the *LQ inverse* problem, extensively discussed in the Sixties and Seventies and which consisted in finding the LQ cost whose minimization restores a given state feedback. This CSF used as such is not of interest since it is necessary to know gains K_c and K_f and the Youla parameter $Q(z)$ to set up the problem $P(z)$ and to finally find the initial augmented LQG compensator. On the other hand, from an arbitrary compensator satisfying some time-domain specifications, one can compute an observer-based realization (i.e. K_c, K_f and $Q(z)$) of this compensator using the technique in Alazard and Apkarian (1999). The CSF is then immediately useful to initialize a standard setup which will be completed by dynamic weighting functions to take into account frequency-domain specifications. In the following application, the CSF is used to embeding a pure discrete-time LQG compensator designed to meet time domain performance. Thus, the initial compensator is already an observer-based realization and the CSF will be applied with $Q(z) = 0$.

3. Launcher control problem

3.1. Description

This application considers the launcher inner control loop.

According to Fig. 3, the following notation is used:

G: the center of gravity,
i: the launcher angle of attack,
ψ: the deviation angle around axis w.r.t. the guidance attitude reference,
V_a and V_r: respectively, the absolute and the relative velocity,
w: the wind velocity,
β: the thruster angle of deflection,
$\dot{z}$: the lateral drift rate.

The rigid behavior is modeled by a third-order system with state vector: $x^r = [\psi\ \dot{\psi}\ \dot{z}]^{\mathrm{T}}$. This rigid model strongly depends on 2 uncertain dynamic parameters A_6 (aerodynamic efficiency) and K_1 (thruster efficiency).

From Fig. 3 and under small angle assumption, one can derive the angle-of-attack equations:

$$i = \psi + \frac{\dot{z} - w}{V}. \tag{12}$$

The discrete-time validation model considered in this paper (that is the full-order model $G_f(z)$) is characterized by the rigid dynamics, the dynamics of thrusters (order 2), sensors (order 2) and the first 5 bending modes (order 10). The launcher is aerodynamically unstable. Finally, the characteristics of bending modes are uncertain (4 uncertain parameters per mode).

3.2. Objectives

The available measurements are the attitude angle (ψ) and rate ($\dot{\psi}$). The control signal is the thruster deflection angle β. Launcher control objectives for the whole atmospheric flight phase are as follows:

- performance with respect to disturbances (wind): the angle of attack peak, in response to the typical wind profile $w(t)$, must stay within a narrow band ($\pm i_{\max}$). This wind profile is plotted in Fig. 4 (dashed plot) and corresponds to a worst case wind encountered during launches with a strong gust when aerodynamic pressure is maximal,
- closed-loop stability with sufficient stability margins. This involves constraints on the rigid mode but also on the flexible modes. In fact, the first flexible mode is "naturally" phase controlled (collocation between sensors and actuator) while the other flexible modes must be gain controlled (roll-off). So, the peaks associated with the flexible modes (except for the first) on the frequency response of the loop gain ($L(s) = K(s)G(s)$) must stay below a specified level X_{dB} for all parametric configurations (see Fig. 9 as an example). From the synthesis point of view, the flexible modes are not taken into account in the synthesis model. But a roll-off behavior with a cut-off frequency between the first and the second flexible modes must be specified in the synthesis,
- delay margin must be greater than one sampling period.

All these objectives must be achieved for all configurations in the uncertain parameter space (22 uncertain parameters including aerodynamics coefficient, propulsion efficiency and bending modes characteristics), particularly in some identified worst cases where the combination of parameter extremal values is particularly critical. In this paper, the robustness analysis is limited to these worst cases as the experience has shown that they are quite representative of the robustness

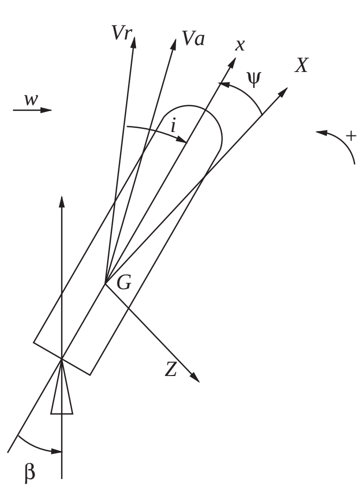

Fig. 3. Launcher simplified representation.

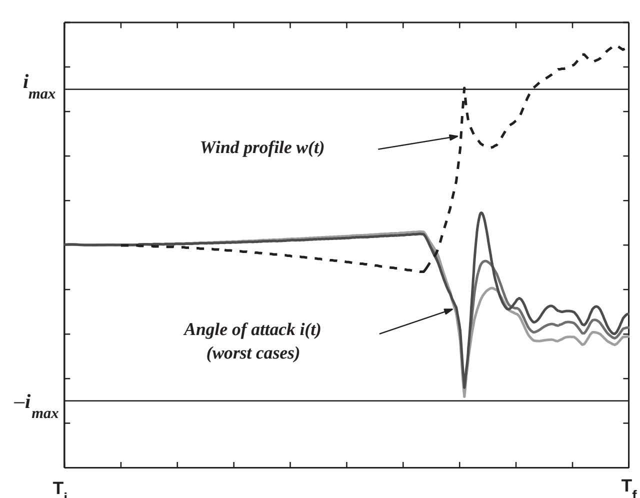

Fig. 4. Angle of attack $i(t)$ (solid) obtained with $K_1(z)$ and wind profile $w(t)$ (dashed, normalized unit).

problem. A more complete μ-analysis is presented in Imbert (2001).

4. Launcher control design

The approach proposed to satisfy all these stationary objectives proceeds in 2 steps: the first one aims to satisfy time-domain specification (angle-of-attack constraint) and the second one is a H_∞ synthesis based on the CSF allowing the frequency-domain specifications (roll-off, stability margins) to be met.

The models used for the synthesis are discrete models including a zero-order hold. The computation of the first step of the synthesis is directly derived from the continuous time synthesis (Voinot et al., 2001).

4.1. First synthesis: non-conventional LQG/LTR synthesis

4.1.1. State feedback on the rigid model

The rigid problem is characterized by 2 controlled outputs i and $\dot{z}$, 2 measurements ψ and $\dot{\psi}$, 1 control signal β and 1 exogenous input w (disturbance). This standard problem reads:

$$\begin{bmatrix} \dot{x}^r \\ \hline i \\ \dot{z} \\ \hline \psi \\ \dot{\psi} \end{bmatrix} = \left[\begin{array}{c|c|c} A & B_1 & B_2 \\ \hline C_1 & D_{11} & D_{12} \\ \hline C_2 & D_{21} & D_{22} \end{array}\right] \begin{bmatrix} x^r \\ \hline w \\ \hline \beta \end{bmatrix}. \tag{13}$$

Then, the gain K_d is computed such that the discrete control law $\beta_k = -K_d x_k^r$ minimizes the following continuous-time LQ criterium:

$$\begin{aligned} J &= \int_0^\infty (\alpha \dot{z}^2 + i^2 + r\beta^2)\, \mathrm{d}t \\ &= \int_0^\infty (x^{r^\mathrm{T}} Q x^r + \beta^\mathrm{T} R \beta + 2 x^{r^\mathrm{T}} N \beta)\, \mathrm{d}t, \end{aligned} \tag{14}$$

with

$$Q = C_1^\mathrm{T} \begin{bmatrix} 1 & 0 \\ 0 & \alpha \end{bmatrix} C_1, \quad R = r, \quad N = 0_{3\times 1}.$$

The model and the performance index are discretized by taking into account the zero-order hold at the input β_k

$$J_d = \sum_{k=1}^{\infty} (x_k^{r\mathrm{T}} Q_d x_k^r + \beta_k^\mathrm{T} R_d \beta_k + 2 x_k^{r\mathrm{T}} N_d \beta_k) \tag{15}$$

for the discrete-time model $x_{k+1}^r = A_d x_k^r + B_{2_d} \beta_k$. The matrices ($A_d$, B_{2_d}, Q_d, N_d and R_d) involving the matrix exponential are computed using the Van Loan's Formula (Loan, 1978).

Adopting the notation

$$K_d = [K_\psi, K_{\dot{\psi}}, K_{\dot{z}}], \tag{16}$$

the gain K_d can be used to build a servo-loop of the measured variable ψ, that is

$$\beta_k = K_\psi(\psi_{\mathrm{ref}_k} - \psi_k) - K_{\dot{\psi}} \dot{\psi}_k - K_{\dot{z}} \dot{z}_k \tag{17}$$

where ψ_{ref_k} is the input reference.

4.1.2. Augmented state with wind dynamic

The wind dynamics is modelled by a stable first-order filter and is then discretized with the zero-order hold method

$$w_{k+1} = A_w w_k + \tilde{w}_k.$$

This disturbance feed-forward model introduces a new tuning parameter A_w. The discrete-time augmented problem corresponding to the state vector $x^a = [x^{r\mathrm{T}}, w]^\mathrm{T}$ then reads

$$\begin{aligned} \begin{bmatrix} x_{k+1}^a \\ \hline i_k \\ \dot{z}_k \\ \hline \psi_k \\ \dot{\psi}_k \end{bmatrix} &= \left[\begin{array}{cc|c|c} A_d & B_{1_d} & 0 & B_{2_d} \\ 0 & A_w & I & 0 \\ \hline C_1 & D_{11} & 0 & D_{12} \\ \hline C_2 & D_{21} & 0 & D_{22} \end{array}\right] \begin{bmatrix} x_k^a \\ \hline \tilde{w}_k \\ \hline \beta_k \end{bmatrix} \\ &= \left[\begin{array}{c|c|c} A_d^a & B_{1_d}^a & B_{2_d}^a \\ \hline C_1^a & 0 & D_{12} \\ \hline C_2^a & 0 & D_{22} \end{array}\right] \begin{bmatrix} x_k^a \\ \hline \tilde{w}_k \\ \hline \beta_k \end{bmatrix} \end{aligned} \tag{18}$$

with $B_{1_d} = \int_0^{T_s} e^{A\eta} B_1 \, \mathrm{d}\eta$.

In order to compute the new state feedback gain K_d^a associated with the augmented state x^a, eq. (17) is used with ψ_{ref_k} such that the angle-of-attack due to disturbance w is cancelled (see eq. (12)), that is

$$\psi_{\mathrm{ref}_k} = \frac{w_k - \dot{z}_k}{V}.$$

Then, the term $\dot{z}_k/V$ is ignored because it can introduce non-stabilizing couplings in the lateral motion. Finally, the gain K_d^a is obtained as

$$K_d^a = \left[K_d, -\frac{K_\psi}{V}\right]. \tag{19}$$

Following this procedure, the LQ state feedback closed-loop dynamics is stable and satisfies:

$$\mathrm{spec}(A_d^a - B_{2_d}^a K_d^a) = \mathrm{spec}(A_d - B_{2_d} K_d) \cup \mathrm{spec}(A_w)$$

4.1.3. Kalman's filter with LTR tuning

To compute the gain G_d^a of the Kalman's filter on the augmented model (A_d^a, $B_{2_d}^a$, C_2^a, D_{22}), an LTR tuning is proposed. It is well known that stability margins of the LQ state feedback are degraded when the Kalman's filter is introduced in the control loop. The LTR procedure allows these stability margins to be recovered (Athans, 1986). Thus, the state noise is composed of 2 disturbing signals: one on the wind model input ($\tilde{w}$) and the other on the control input β through a gain $\sqrt{\rho}$

(LTR effect)

$$W = \begin{bmatrix} \rho B_2 B_2^T & 0 \\ 0 & I \end{bmatrix} \text{ and } V = v \begin{bmatrix} 1 & 0 \\ 0 & \omega_f^2 \end{bmatrix}$$

W and V are the covariance matrices of continuous-time noises on the state vector (x^a) and the measurement vector ($[\psi, \dot{\psi}]^T$), respectively. Therefore, the KALMAN filter tuning depends on 3 parameters: ρ (LTR weighting), v (measurement to state noise ratio) and $\omega_f(rd/s)$ (rate to position measurement noise ratio), ω_f represents the frequency beyond which it is better to integrate the rate measurement $\dot{\psi}$ to estimate the position $\hat{\psi}$ than to use the measurement position ψ directly.

The covariance matrices, W_d and V_d, of discrete-time noises on the state vector and the measurement vector are also discretized using Van Loan's formulae.

This non conventional LQG/LTR design yields a fourth-order compensator $K_1(z)$ involving the gains K_d^a and G_a^d and the augmented model (A_d^a, $B_{2_d}^a$, C_2^a, D_{22}) and defined by equation (2) without YOULA parameter $Q(z)$. The results obtained so far are presented in Figs. 4 and 5.

In Fig. 4 it can be observed that the performance requirements (angle-of-attack) are quite satisfied for all worst cases. In Fig. 5, one can also note that the template for low frequency stability margins is satisfied (this templates is depicted in Fig. 5 with the vertical line on the first critical point on the right-hand side) and the first flexible mode remains between two critical points for all worst cases (phase control). But the roll-off effect is not strong enough: the template for gain margins on flexible modes number 2 and 3 (depicted in Fig. 5 with the horizontal line at X_{dB}) is not satisfied in any case. Note that NICHOLS plots are obtained with discrete-time transfers: it appears that flexible modes 4 and 5 are aliasing between flexible modes 1 and 3. These modes are not significant for the control design.

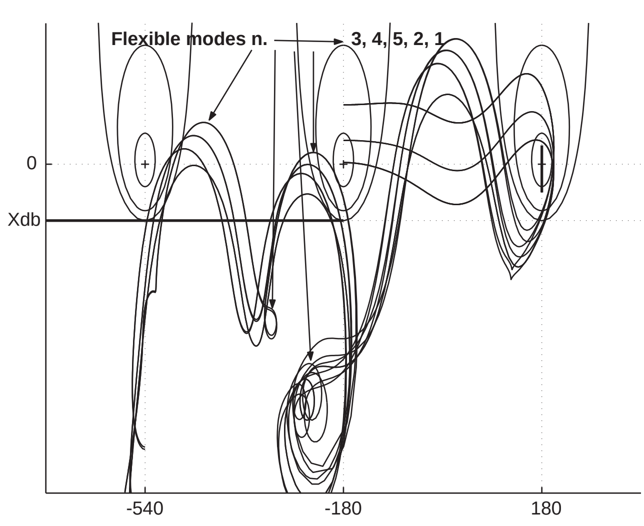

Fig. 5. $K_1(z)G_f(z)$: NICHOLS's plots for worst cases.

4.2. *Second synthesis: H_∞ synthesis using CSF for frequency-domain specifications*

In order to satisfy this last frequency domain requirement, an H_∞ synthesis is performed on the standard problem depicted in Fig. 6:

This standard problem can be described as follows:

- between inputs e and u and outputs q_2 and y, one can recognize the CSF presented in Section 2.2 which will inflect the solution towards the previous pure performance compensator (LQG/LTR design),
- the output q_1 is introduced to specify the roll-off behavior with a second-order filter $F(z)$ in order to fulfil the gain margin template on flexible modes number 2 and 3.

The output q_1 in fact, weighs the second-order derivative of the control signal u. The frequency domain response of $F(z)$ is depicted in Fig. 7. This response exhibits a wide hump centered on the flexible modes 2 and 3. This hump frames peak variations of flexible modes 2 and 3 for all worst cases.

Then, the H_∞ synthesis provides a sixth-order compensator $K_2(z)$. Analysis results are displayed in Figs. 8 and 9. The time-domain performance specification is still met (Fig. 8). Fig. 9 shows that stability margins are good enough for all worst cases and the roll-off behavior is now quite satisfactory.

5. Gain-scheduling

The previous stationary design has been applied for various instants t^i along the flight envelope. The H_∞ solver which has been used is the Matlab macro-function `dhinfric` because it provides the best index γ

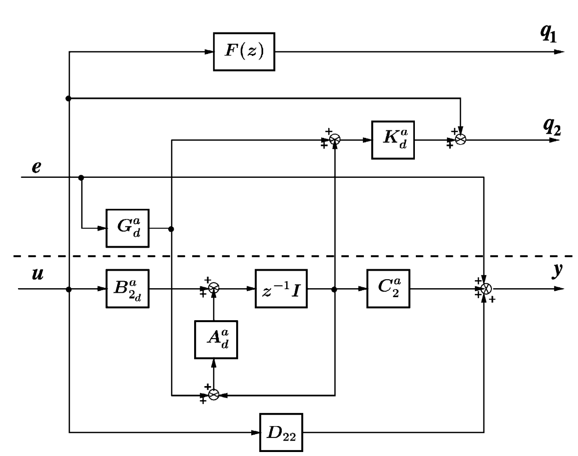

Fig. 6. $P_f(z)$: setup for the final H_∞ synthesis.

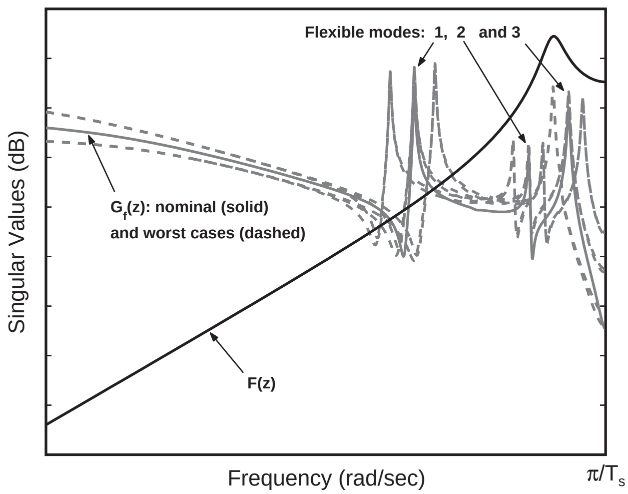

Fig. 7. Singular values: $F(z)$ (black) and $G_f(z)$ (grey).

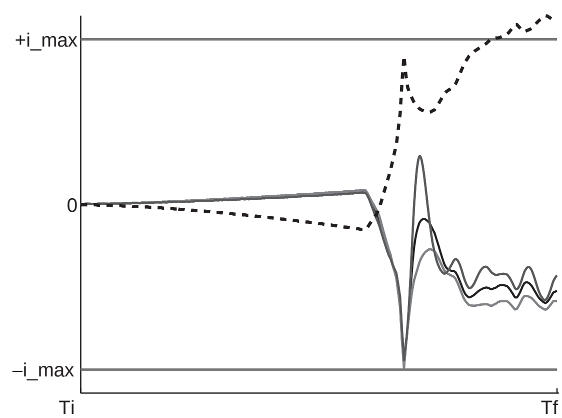

Fig. 8. Angle of attack $i(t)$ (solid) obtained with $K_2(z)$ and wind profile $w(t)$ (dashed).

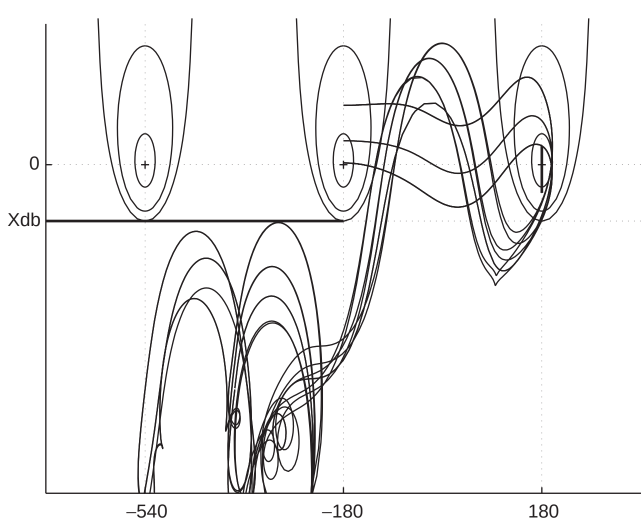

Fig. 9. $K_2(z)G_f(z)$: NICHOLS plot for worst cases.

among the various algorithms proposed in the various Matlab toolboxes. The drawback of this algorithm lies in the fact that the solution $K_2^i(z)$ is not the central DGKF solution. Because of multiple variable changes performed to increase numerical conditioning in Riccati equations, the realization of the solution has no physical meaning. The linear interpolation of the four matrices (A_K^i, B_K^i, C_K^i and D_K^i) provides a non-stationary compensator noted $K_2(z,t)$ with an awkward behavior as can be seen from the evolution of the singular value of $K_2(z,t)$ as a function of time t during the atmospheric flight (Fig. 10).

This problem can be easily mastered using observer-based realizations. Thus, an observer-based realization of each compensator $K_2^i(z)$ is computed using the approach presented in Alazard and Apkarian (1999). The model used in this realization is the transfer between u and y of the standard problem $P_f(z)$ (see Fig. 6). The main difficulty with this approach is that the observer-based realization is not unique and depends on the way the closed-loop dynamics $F_l(P_f^i(z), K_2^i(z))$ is split between the state feedback dynamics and the state estimation dynamics. Considering the particular structure of the standard problem $P_f(z)$, this difficulty is easily overcame:

Let $\left[\begin{array}{c|c} A_F & B_F \\ \hline C_F & D_F \end{array}\right]$ be a realization of the weighting filter $F(z)$, then the realization of the augmented plant $P_f(z)$ depicted in Fig. 6 is given as

$$P_f(z) := \left[\begin{array}{cc|c|c} A_d^a & 0 & A_d^a G_d^a & B_{2_d}^a \\ 0 & A_F & 0 & F_F \\ \hline 0 & C_F & 0 & D_F \\ K_d^a & 0 & K_d^a G_d^a & 1 \\ \hline C_2^a & 0 & I_{2\times 2} & D_{22} \end{array}\right] = \left[\begin{array}{c|c|c} \mathscr{A} & \mathscr{B}_1 & \mathscr{B}_2 \\ \hline \mathscr{C}_1 & \mathscr{D}_{11} & \mathscr{D}_{12} \\ \hline \mathscr{C}_2 & I_{2\times 2} & D_{22} \end{array}\right].$$

One can also derive

$$\mathrm{spec}(\mathscr{A} - \mathscr{B}_1\mathscr{C}_2) = \mathrm{spec}(A_d^a(I - G_d^a C_2^a)) \cup \mathrm{spec}(A_F).$$

The first term ($\mathrm{spec}(A_d^a(I - G_d^a C_2^a))$) represents the stable dynamics of the Kalman filter previously designed. The second term ($\mathrm{spec}(A_F)$) stands for the roll-off filter

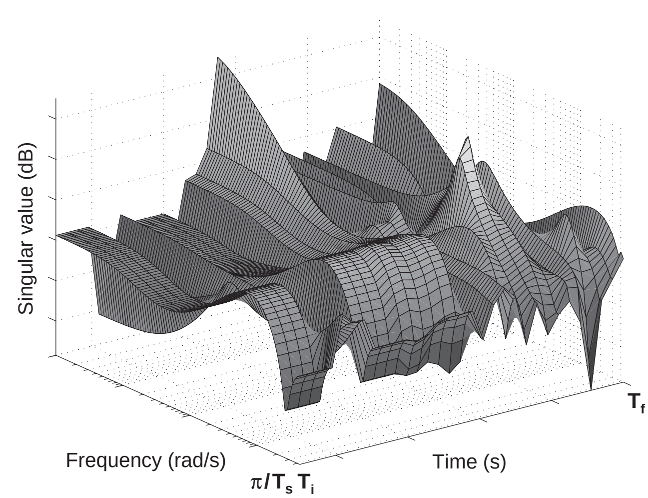

Fig. 10. $K_2(z,t)$: singular value w.r.t. time.

dynamics which must be chosen stable. From Appendix A, it can be derived that our standard problem $P_f(z)$ is a pure Disturbance Feed-forward (DF) problem and that half of the closed-loop dynamics of $F_l(P_f(z),K_2(z))$ will be assigned to spec($\mathscr{A} - \mathscr{B}_2\mathscr{C}_2$) for any value of the final index γ. This dynamics must be assigned to the state estimation dynamics when one wants to find the equivalent observer-based compensator $K_2(z)$ using the algorithm proposed in Alazard and Apkarian (1999). Then, the observer-based realization becomes unique.

Let us note

$$\left[\begin{array}{c|c} A^i_{LQG} & B^i_{LQG} \\ \hline C^i_{LQG} & D^i_{LQG} \end{array}\right]$$

$$= \left[\begin{array}{c|c} \mathscr{A} - \mathscr{B}^i_2\mathscr{K}^i_s - \mathscr{K}^i_f\mathscr{C}^i_2 + \mathscr{K}^i_f\mathscr{D}^i_{22}\mathscr{K}^i_\varepsilon & \mathscr{K}^i_f \\ \hline \mathscr{K}^i_\varepsilon & \mathscr{D}_Q \end{array}\right]$$

the observer-based realization of each compensator $K^i_2(z)$. The linear interpolation of the four new matrices (A^i_{LQG}, B^i_{LQG}, C^i_{LQG} and D^i_{LQG}) provides a new non-stationary compensator noted $K_{LQG}(z,t)$. The evolution of the singular value of $K_{LQG}(z,t)$ w.r.t. time t is presented in Fig. 11. This response is significantly smoother than the one of Fig. 10.

Fig. 12 depicts the evolution of the stability margins during the whole atmospheric flight for all worst cases. Obtained margin to desired margin ratios (in percent) are plotted w.r.t. time for the low frequency gain margin (LF margin: above the right-hand critical point in the Nichols chart), the high frequency gain margin (HF margin: under the right-hand critical point in the Nichols chart), the attenuation of the flexible modes below X_{dB} (corresponding to horizontal line in the Nichols chart) and the delay margin. One can notice that the specifications are met at each instant of the flight (ratios must be positive to fulfil specifications).

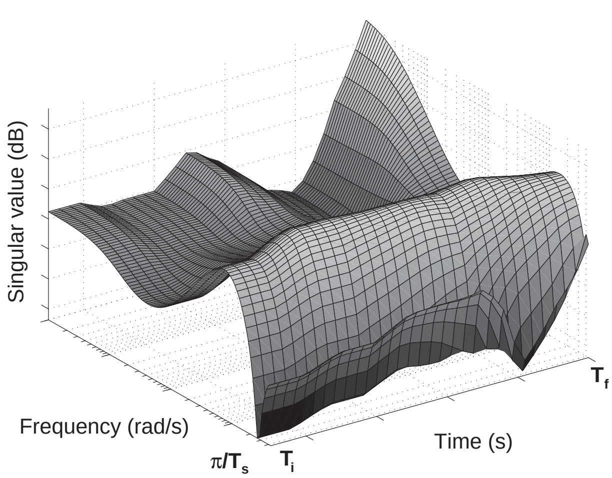

Fig. 11. $K_{LQG}(z,t)$: singular value w.r.t. time.

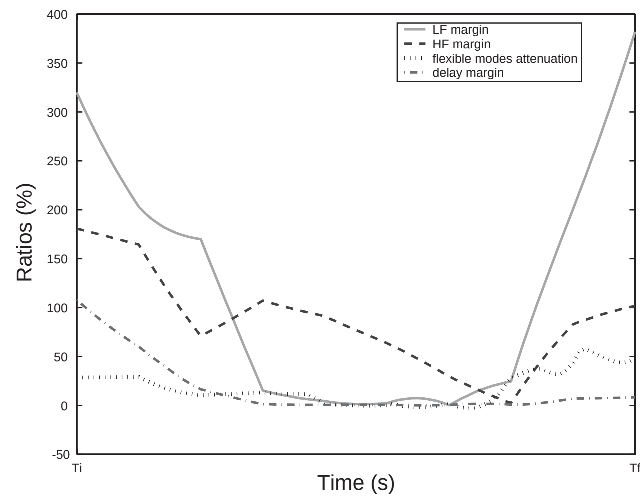

Fig. 12. Obtained margin to desired margin ratios w.r.t. time.

6. Conclusion

The multi-objective synthesis approach based on the Cross Standard Form (CSF) presented in this paper gives interesting results on the launcher problem. It has been shown that the CSF leads to a very specific synthesis setup in which a priori knowledge can be easily captured. Because of the particular 2 steps computation of the gain K^a_d (see eq. (19)), it is not possible to build directly a standard (H_2 or H_∞) problem equivalent to this non-conventional LQG/LTR design. The use of the CSF overcomes this problem.

On the non-stationary problem, the interest of observer-based structure to obtain a smooth gain-scheduling is highlighted. The computation of observer-based realizations of each stationary compensator is straightforward when regarded as a pure Disturbance Feed-forward structure of the final H_∞ problem.

Appendix A. The disturbance feed-forward problem

The Disturbance Feed-forward DF problem is discussed in Zhou et al., (1996) with some additional normalization assumptions. The results presented here are performed in continuous-time domain for clarity but can be transformed to the discrete-time case. The realization of the general DF problem is taken to be of the form:

$$P(s) = \left[\begin{array}{c|cc} A & B_1 & B_2 \\ \hline C_1 & D_{11} & D_{12} \\ C_2 & I & D_{22} \end{array}\right] \qquad \text{(A.1)}$$

with the followings assumptions:

1. (A, B_1) is stabilizable and (C_1, A) is detectable.
2. (A, B_2) is stabilizable and (C_2, A) is detectable.
3. $A - B_1C_2$ is stable.

The central sub-optimal compensator $K(s)$ such that $\|F_l(P, K\|_\infty < \gamma$ involves the solutions X_∞ and Y_∞ of two coupled Riccati equation associated with the following Hamiltonian matrices (Zhou et al., 1996):

$$H_\infty = \begin{bmatrix} A & 0 \\ -C_1^T C_1 & -A^T \end{bmatrix} + \begin{bmatrix} B_1 & B_2 \\ -C_1^T D_{11} & -C_1^T D_{12} \end{bmatrix} \times \begin{bmatrix} \gamma^2 I - D_{11}^T D_{11} & -D_{11}^T D_{12} \\ -D_{12}^T D_{11} & -D_{12}^T D_{12} \end{bmatrix}^{-1} \begin{bmatrix} D_{11}^T C_1 & B_1^T \\ D_{12}^T C_1 & B_2^T \end{bmatrix}, \tag{A.2}$$

$$J_\infty = \begin{bmatrix} A^T & 0 \\ -B_1 B_1^T & -A \end{bmatrix} + \begin{bmatrix} C_1^T & C_2^T \\ -B_1 D_{11}^T & -B_1 \end{bmatrix} \times \begin{bmatrix} \gamma^2 I - D_{11} D_{11}^T & -D_{11} \\ -D_{11}^T & -I \end{bmatrix}^{-1} \begin{bmatrix} D_{11} B_1^T & C_1 \\ B_1^T & C_2 \end{bmatrix}. \tag{A.3}$$

The development of J_∞ leads to

$$J_\infty = \begin{bmatrix} (A - B_1 C_2)^T & * \\ 0 & -(A - B_1 C_2) \end{bmatrix}. \tag{A.4}$$

As $A–B_1C_2$ is stable, the solution of the associated Ricatti equation is null for any value of γ:

$$Y_\infty = 0.$$

Then, the condition $\rho(X_\infty Y_\infty) < \gamma^2$ is always satisfied for any value of γ and the central solution (with the choice $D_c = 0$ in the Parrott problem) has the following observer-based form:

$$K_\infty(s) : \left[\begin{array}{c|c} A_c & B_c \\ \hline C_c & D_c \end{array}\right] = \left[\begin{array}{c|c} A - B_2 K - G C_2 + G D_{22} K & G \\ \hline -K & 0 \end{array}\right] \tag{A.5}$$

with

- $K = D_{12}^{+}(D_{12}^{+T} B_2^T X_\infty + C_1)$,
- $G = B_1$,
- and the notation : $M^{+} = (M^T M)^{-1} M^T$.

So, for any value of γ, the H_∞ sub-optimal central compensator on the problem (eq. (A.1)) is a *pure observer-based compensator* on the model (A, B_2, C_2, D_{22}). Only, the state feedback gain depends on γ. The closed-loop dynamics of $F_l(P(s)K(s))$ is split between spec($A–B_1C_2$) (independent of γ) and spec($A–B_2K$) (dependent on γ).

References

Alazard, D. (2002). Robust H_2 design for lateral flight control of a highly flexible aircraft. *Journal of Guidance, Control, and Dynamics*, *25*(6), 502–509.

Alazard, D., & Voinot, O. (2002). Cross standard form for generalized inverse problem: Application in robust control. *Submitted for publication.*

Alazard, D., & Apkarian, P. (1999). Exact oberserver-based structures for arbitrary compensators. *International Journal of Robust and Non-Linear Control*, *9*, 101–118.

Apkarian, P., Tuan, H. D., & Bernussou, J. (2001). Continuous-time analysis, eigenstructure assignment and H_2 multi-channel synthesis with enhanced LMI characterizations. *IEEE Transactions on Automatic Control*, *46*(12), 1941–1946.

Athans, M. (1986). A tutorial on the lqg/ltr method. In: *Proceedings of American control conference.* IEEE, Seattle (WA). pp. 1289–1296.

Clément, B., & Duc, G. (2000). A multi-objective control algorithm: Application to a launcher with bending modes. In: *18th IEEE Mediterranean Conference on Control and Automation*, Patras.

Clément, B., Duc, G., Mauffrey, S., & Biard, A. (2001). Gain scheduling for an aerospace launcher with bending modes. In: *15th IFAC symposium on automatic control in aerospace*, Bologna.

Doyle, J., Glover, K., Khargonekar, P. P., & Francis, B. A. (1989). State-space solutions to standard H_2 and H_∞ control problems. *IEEE Transactions on Automatic Control*, *34*, 831–847.

Doyle, J., Zhou, K., Glover, K., & Bodenheimer, B. (1994). Mixed H_2 and H_∞ performance—objectives *II*: Optimal control. *IEEE Transactions on Automatic Control*, *39*, 1575–1587.

Fan, Y., Cliff, E. M., Lutze, F. H., & Anderson, M. R. (1996). Mixed H_2/H_∞ optimal control for an elastic aircraft. *Journal of Guidance, Control, and Dynamics*, *19*, 650–655.

Griffin, I. A., Schroder, P., Chipperfiled, A. J., & Fleming, P. J. (2000). Multiobjective optimization approach to the alstom gasifier control. *Special Issue of the Institution of Mechanical Engineers, Part I, Journal of Systems and Control Engineering*, *214*(I6), 453–468.

Imbert, N. (2001). Robustness analysis of a launcher attitude controller via μ-analysis. In: *15th IFAC Symposium on Automatic Control in Aerospace*, Bologna.

Loan, C. F. Van, 1978. Computing integrals involving the matrix exponential. *IEEE Transactions on Automatic Control*, AC-*23*(3), 395–404.

Mauffrey, S., & Scholler, M. (1998). Non-stationary H_∞ control for launcher with bending modes. In: *14 IFAC symposium on automatic control in aerospace*, Séoul.

Pellanda, P.C., Apkarian, P., & Alazard, D. (2000). Gain-scheduling through continuation of observer-based realizations—applications to H_∞ and μ controllers. In: *Proceedings of the 39th IEEE conference decision and control*, IEEE, Sydney, pp. 2787–2792.

Shue, S.-P., & Agarwal, R. K. (1999). Design of automatic landing systems using mixed $\mathcal{H}_2/\mathcal{H}_\infty$ control. *Journal of Guidance, Control, and Dynamics*, *22*, 103–114.

Stilwell, D. J., & Rugh, W. (1999). Interpolation of observer state feedback controllers for gain scheduling. *IEEE Trans. Automatic Control*, *44*(6), 1225–1229.

Voinot, O., Alazard, D., Piquereau, A., & Biard, A. (2001). A robust multi-objective synthesis applied to launcher attitude control. In: *15th IFAC symposium on automatic control in aerospace*, Bologna.

Zhou, K., Doyle, J. C., & Glover, K. (1996). *Robust and optimal control.* Englewood Cliffs, NJ: Prentice-Hall.